 CMC, vol.17, no.1, pp.1-17, 2010

Topology of Homophase Grain Boundaries in Two-Dimensional Crystals: The Role of Grain Exchange Symmetry

S. Patala[1] **and C.A. Schuh**[1]

Abstract: Recent advances in microstructural characterization have made it possible to measure grain boundaries and their networks in full crystallographic detail. Statistical studies of the complete boundary space using full crystallographic parameters (misorientations and boundary plane inclinations) are limited because the topology of the parameter space is not understood (especially for homophase grain boundaries). This paper addresses some of the complexities associated with the group space of grain boundaries, and resolves the topology of the complete boundary space for systems of two-dimensional crystals. Although the space of homophase boundaries is complicated by the existence of a 'no-boundary' singularity, i.e., no boundary exists when the misorientation is zero, here it is shown that this singularity can be removed owing to a second special symmetry. Specifically, "grain exchange symmetry" refers to the indistinguishability of the adjoining grains at a homophase boundary, and results in symmetrically equivalent descriptions of the boundary. This symmetry affects the topology of misorientation spaces, removes the 'no-boundary' singularity, and permits the identification of the space topology for two-dimensional crystals with various point symmetries. For crystals of C_1 and C_3 point symmetry, the homophase grain boundary space is shown to be D^2, while for C_2, C_4, and C_6 symmetries it is $\mathbb{R}P^1$.

Keywords: Grain Boundaries, Topology

1 Introduction

Grain boundaries constitute an important component of structure in polycrystalline materials, and have a profound influence on those properties that depend either upon transgranular (Argon and Qiao 2002; Ju, Sun, and Li 2002; Kraft and Molinari 2008) or intergranular phenomena (Lim and Watanabe 1990; Aust, Erb, and

[1] Department of Materials Science and Engineering, Massachusetts Institute of Technology, Cambridge, MA USA 02139

Palumbo 1994; Watanabe 1994; Kokawa, Shimada, Michiuchi, Wang, and Sato 2007). Grain boundaries are characterized by crystallographic parameters describing the rotational difference (misorientation) between adjoining grains, as well as the boundary plane, or inclination. Advances in automated serial sectioning methods, combined with local crystallographic measurements by electron backscatter diffraction, allow the measurement of these parameters for large numbers of grain boundaries in three dimensions (Rowenhorst, Gupta, Feng, and Spanos 2006; Uchic, Groeber, Dimiduk, and Simmons 2006; Groeber, Haley, Uchic, Dimiduk, and Ghosh 2006; Spowart 2006). Studies investigating the relationship between properties, energetics and structure of grain boundaries as a function these crystallographic parameters are consequently on the rise (Kim, Rollett, and Rohrer 2006; Rohrer, Saylor, El Dasher, Adams, Rollett, and Wynblatt 2004; Olmsted, Foiles, and Holm 2009; Olmsted, Holm, and Foiles 2009).

Despite these remarkable characterization advances, our theoretical understanding of the complete grain boundary space remains very limited. For a quantitative analysis of statistics or dynamics of grain boundaries, it is necessary to understand the topology of the five-dimensional space in which the crystallographic parameters describing the grain boundaries reside. The space of misorientations (denoted as $\mathbf{M}$) is the quotient space of rotations $(SO(3))$ obtained by applying equivalence relations that arise due to underlying crystal symmetries. And similarly the space of boundary inclinations (denoted as $\mathbf{B}$) is the quotient space of unit normal vectors (represented by points on the surface of a unit sphere S^2). Since the complete boundary inclination space $\left(S^2\right)$ is accessible for any given boundary misorientation, the topology of the complete boundary space (denoted as $\mathscr{M}$) is the *product space* of misorientations $(SO(3))$ and boundary inclinations $\left(S^2\right)$, i.e. $\mathscr{M} \equiv \mathbf{M} \times \mathbf{B} \equiv SO(3) \times S^2$, with proper symmetries applied (Morawiec 2009).

The product space $SO(3) \times S^2$ is well understood, and metrics and measures on this space have been recently developed (Morawiec 2009). However, this product space is not the complete picture for grain boundaries; it strictly applies only to heterophase boundaries and not to homophase grain boundaries, which are distinct. The distinction is due to the zero misorientation ($\mathbf{M} = I$, with I being the zero misorientation) boundaries. For heterophase boundaries, at $\mathbf{M} = I$ there still exists a physical boundary that separates the two phases, and thus different boundary inclinations are physically distinguishable. This makes the analysis of such boundaries straightforward on the product space $SO(3) \times S^2$. In contrast, in the case of homophase boundaries, no misorientation implies that there is no grain boundary at all; there are no additional inclination degrees of freedom for $\mathbf{M} = I$. Therefore, the topology of $\mathscr{M}$ for homophase boundaries is the product space $SO(3) \times S^2$ with the significant added caveat that all the boundary inclinations at $\mathbf{M} = I$ are identified.

Due to the equivalence of boundary inclinations for the zero misorientation case, the topology of the homophase boundary space remains unclear. One possible approach to handling this difficulty is to employ the heterophase boundary space but with warped product metrics that account for the singularity at $\mathbf{M} = I$. However, this approach has drawbacks arising from arbitrary choice of the scaling function (Morawiec 2009). The 'no-boundary' (zero misorientation) region is important because it affects how the distance between low-angle grain boundaries is defined (Olmsted 2009). As discussed by Cahn and Taylor (2006) the 'no-boundary' singularity in boundary description plays an important role in determining appropriate metrics and topology for homophase systems.

In addition to the 'no-boundary' case in homophase boundaries, there exists a special symmetry that distinguishes the description of homophase boundaries from the heterophase case. Since the two adjoining grains that define a homophase interface are not physically distinguishable, the crystallographic parameters measured with respect to the reference frame of one grain are equivalent to those measured with respect to the other grain. This equivalence relation, which we refer to as 'grain exchange symmetry', is expressed mathematically as

$$(\mathbf{M}, \mathbf{n}) \sim \left(\mathbf{M}^{-1}, \mathbf{M}^{-1}(-\mathbf{n})\right) \tag{1}$$

In this paper we demonstrate the importance of this equivalence relation in understanding the topology of homophase boundary space. As a means of highlighting a variety of different implications of Equation 1, we limit our discussion to two-dimensional systems, i.e., 1D linear boundaries between 2D crystals. This simple problem has all of the critical features of the full 3D problem, but permits visualization of the results in a far more transparent manner, and provides a useful first step towards solution of the full 3D problem. First we consider the effect of the grain exchange symmetry relation on the topology of misorientation space, and then describe how this relation helps identify the topology of the complete boundary space.

2 Two-dimensional rotation space

We first consider the effect of the grain exchange symmetry on *connectivity* in two-dimensional rotation space. Two dimensional rotations correspond to rotations around a fixed axis. Without loss of generality, we consider the axis of rotation to be the z-axis and the crystals being rotated to reside in the x-y plane. There exist various parameterizations of the 2D rotation space:

(i) Any rotation operation in two-dimensions can be specified by the angle of rotation $\omega \in [0, 2\pi)$ about the z-axis.

(ii) There exists a one-to-one correspondence between 2D rotations and $SO(2)$ matrices (2×2 special orthogonal matrices), which can therefore also be used to specify the rotation.

(iii) $SO(2)$ is homeomorphic to S^1 (one-sphere or a circle), and thus the coordinates on the circle can represent 2D rotations.

Some topological properties of S^1 (the 2D rotation space) include:

a) *Embedding* (Basener 2006, 82): Even though only one independent variable is required to uniquely represent 2D rotations (ω as defined in (i) above), a minimum of two variables (coordinates of the circle as in (iii) above) are required for a one-to-one and continuous representation. The bijective mapping $f : \mathbf{R_{2D}} \rightarrow [0, 2\pi)$, where $\mathbf{R_{2D}}$ represents the 2D rotation space, is not a continuous mapping (Munkres 2000, 107). The discontinuity arises due to the equivalence of the rotations ω and $\omega + 2\pi$. The bijective mappings $f : \mathbf{R_{2D}} \rightarrow SO(2)$ and $f : \mathbf{R_{2D}} \rightarrow S^1$ are continuous with a continuous inverse, which implies a topological equivalence of the 2D rotation space, $SO(2)$ and S^1. $f : \mathbf{R_{2D}} \rightarrow S^1$ represents an *embedding* in $\mathbb{R}^2$ because a circle resides in $\mathbb{R}^2$ (the two dimensional Euclidean plane). S^1 is the quotient space of a line segment with its end points identified. If the domain $\omega = [0, 2\pi)$ is used to represent rotations, the rotations $\{0\}$ and $\{2\pi\}$ are equivalent (connected in a topological sense). The minimum number of Euclidean dimensions required to establish this connectivity is two. Fig. 1(a) is a graphical representation of the rotation space using colors; each color uniquely determines the rotation (one-to-one) and similar colors represent similar rotations (continuity).

b) *Fundamental Group* (Munkres 2000, 322): The fundamental group represents the classes of coterminous paths (those that originate and end at the same point). The 2D rotation space has a non-trivial fundamental group, which is to say that there exist coterminous paths that cannot be continuously deformed into a single point. The 2D rotation space is homeomorphic to a circle and any coterminous path on a circle covers the entire circle and cannot be deformed into a single point without moving the path out of the circle. The fundamental group of S^1 and hence the 2D rotation space is $\mathbf{Z}$ (the additive group of integers) (Munkres 2000, 368).

3 Misorientation Space

A misorientation is defined as the rotational difference between two adjoining grains. Since rotations are always defined with respect to a reference coordinate

frame, there are two descriptions of the same misorientation depending on the grain chosen as the reference; for two grains A and B the relation $M_{AB} = M_{BA}^{-1}$ holds, with the misorientation with respect to grain A denoted as M_{AB} and that with respect to grain B as M_{BA}. Equivalence relations arise if the adjoining grains A and B have underlying point symmetries and if grains A and B are not physically distinguishable (as in the homophase case). Hence, the misorientation space is the quotient space of the rotation space obtained by applying various equivalence relations. This section deals with the equivalence relations and their effect on the topology of misorientation space.

3.1 Heterophase Misorientation Space

If grains A and B belong to different point groups (for example at a phase boundary in a multiphase alloy), it is necessary to distinguish whether the misorientation is with respect to crystal A or with respect to crystal B (Heinz and Neumann 1991), and by convention heterophase misorientation is defined with respect to the crystal system of lower symmetry. The symmetrically equivalent descriptions for misorientations are obtained by considering all the symmetrically equivalent orientations of crystals A and B. For example, if phase A is the crystal system with lower symmetry then the following equivalence relations hold:

$$\mathbf{M_{AB}} \sim \left(\mathbf{S_A^i}\right)^{-1} (\mathbf{M_{AB}}) \left(\mathbf{S_B^j}\right);; \quad i = 1,\ldots,n;\ j = 1,\ldots,m \tag{2}$$

where S_A, S_B refer to the point symmetries and n, m refer to the *order* (number of non-equivalent operations constituting a symmetry group) of the point groups of crystals A and B respectively.

The above equivalence relations, when applied to the 2D rotation space and expressed using the ω parameterizations, take the form: $\omega \sim \omega + 2\pi/k$ where $k = l\mathrm{cm}(\mathrm{m},\mathrm{n})$. This relation can be easily checked using the fact that the 2D rotation group is Abelian. In this case the unique representatives of ω (fundamental zone) belong to the interval $[0,\ 2\pi/k)$. The quotient space of rotations obtained after applying this equivalence relation is equivalent to the rotation space with the same connectivity, except that the domain is scaled by k. Thus, from a topological point of view the heterophase misorientation space is equivalent to the 2D rotation space. Fig. 1(b) shows a graphical representation of the heterophase misorientation space of the $C_1 - C_2$ system. It is color coded in a similar fashion to the rotation space in Fig. 1a. The coloring represents the connectivity and the topological equivalence. The topological equivalence implies that the minimum embedding dimension for the heterophase misorientation space is *two* and the fundamental group is $\mathbf{Z}$.

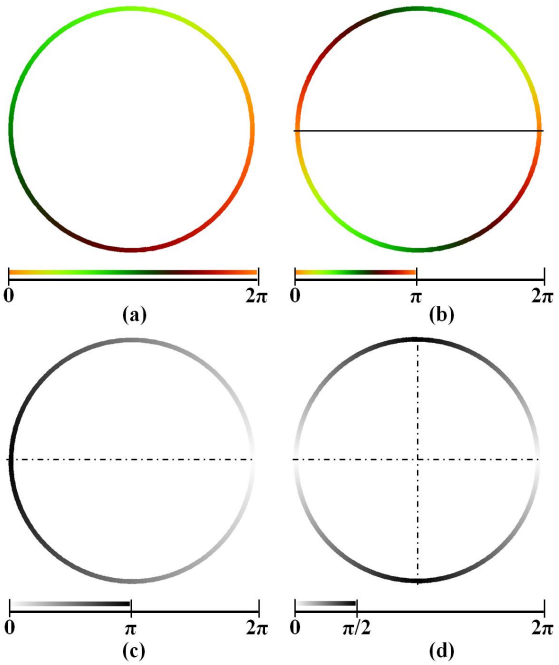

Figure 1: The rotation and misorientation spaces represented on a circle and using the ω parameterization, color coded to show the inherent connectivity of these spaces. (a) The 2D rotation space: $\omega \in [0, 2\pi)$ and the coloring indicates that $\omega \sim 2\pi + \omega$. (b) Misorientation space of $\mathbf{C}_1 - \mathbf{C}_2$ system: $\omega \in [0, \pi)$ and $\omega \sim \pi + \omega$. (a) & (b) are topologically equivalent. (c) Misorientation space of $\mathbf{C}_1 - \mathbf{C}_1$ system: $\omega \in [0, \pi]$ and $\omega \sim 2\pi - \omega$. The crucial difference is that the end points of the domain 0 and π. (d) Misorientation space of $\mathbf{C}_2 - \mathbf{C}_2$ system: $\omega \in [0, \pi/2]$.

3.2 Homophase Misorientation Space

In the case of homophase misorientations, the grain exchange symmetry (Eq. (1)) is added to the equivalence relations:

$$\mathbf{M} \sim \mathbf{M}^{-1} \sim \mathbf{S}_i \mathbf{M} \mathbf{S}_j \sim \mathbf{S}_i \mathbf{M}^{-1} \mathbf{S}_j; \quad i, j = 1, \ldots, n. \tag{3}$$

Since grains A and B are not physically distinguishable when they belong to the same phase, the descriptions M_{AB} and M_{BA} are equivalent. We find that this additional equivalence relation reduces the embedding dimensions for the representation of homophase misorientations and also results in a trivial fundamental group for homophase misorientation space. The above equivalence relations, when ex-

pressed using the ω parameterization, take the following form:

$$(i)\,\omega \sim 2\pi - \omega \quad (ii)\,\omega \sim \frac{2\pi i}{n} + \omega; \quad i = 1,\ldots,n \tag{4}$$

Since the domain for unique representation (the fundamental zone) of the rotation space is $[0,2\pi)$, if only the rotational symmetries are considered the fundamental zone is $[0,2\pi/n)$. But applying the additional grain exchange symmetry equivalence relation reduces the fundamental zone to $[0,\pi/n]$. For any ω greater than π/n there exists an equivalent misorientation $(2\pi/n)-\omega$ in the interval $[0,\pi/n]$. The connectivity in this case is very different from the case of heterophase misorientations. The end points of the fundamental zone ω= 0 and $\omega = \pi/n$ represent distinct misorientations. Hence, the misorientation space represented using ω is a one-to-one and continuous mapping with a continuous inverse. The misorientation space can therefore be embedded in one-dimensional Euclidean space $\mathbb{R}^1$.

The homophase misorientation spaces for systems $C_1 - C_1$ and $C_2 - C_2$ are color coded using only one variable (contrast) as shown in Fig. 1(c&d). The purpose of this illustration is to point out the role of symmetry in the representations. For homophase misorientations, the coloring indicates the presence of mirrors at the boundaries (points in this case) of the fundamental zone. In contrast, for rotation space and heterophase misorientations, the boundaries of the fundamental zone are connected as indicated by the coloring scheme. The homophase misorientation space is equivalent to a closed interval on the real line and admits a trivial fundamental group. Any coterminous path can be continuously deformed into a single point. Hence the grain exchange symmetry leads to a simpler topology of the misorientation space for homophase boundaries.

4 Complete Boundary Space

4.1 Product Space: $\mathbf{S}^1 \times \mathbf{S}^1$

As already discussed, the misorientation space for 2D grain boundaries defined by $\omega \in [0,2\pi)$ is equivalent to S^1 with additional symmetries from the underlying crystals. The boundary inclinations for 2D boundaries are defined by the space of unit vectors in the plane, which belong to the points on S^1 (which can also be represented using $\omega \in [0,2\pi)$). Since the misorientations and inclinations of a boundary are independent, the topology of 2D boundary information is the product space $S^1 \times S^1$ (torus), as illustrated in Fig. 2, with appropriate equivalence relations applied. In the case of homophase boundaries, because of the 'no-boundary' case at zero misorientation, the topology is $S^1 \times S^1$ with the region $\{\omega = 0\} \times S^1$ identified. As it turns out, grain exchange symmetry plays a major role in determining the topology of homophase boundary space, as developed in the following.

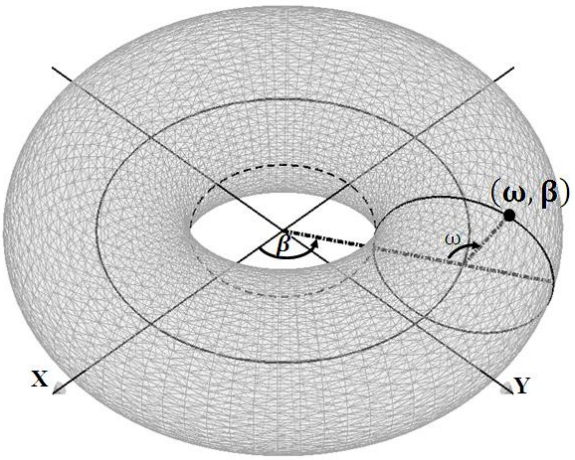

Figure 2: The torus represents the product space $\mathbf{S}^1 \times \mathbf{S}^1$. Any point on the torus can be defined using (ω, β) parameters. Here ω represents the boundary misorientation and β represents the boundary inclination and $\omega, \beta \in [0, 2\pi)$.

4.2 Heterophase Boundaries

The heterophase boundary space is the quotient space of a torus and the equivalence relations consisting of rotational (crystal) symmetry operations. The equivalence relations for the heterophase case are (the same convention as heterophase misorientations is used here) (Morawiec 2004, 129):

$$(\mathbf{M_{AB}}, \mathbf{n_{AB}}) \sim \left(\left(S_A^i\right)^{-1} \mathbf{M_{AB}} \left(S_B^j\right), \left(S_A^i\right)^{-1} \mathbf{n_{AB}} \right); \quad i = 1, \ldots, n;\ j = 1, \ldots, m \tag{5}$$

Expressed in terms of the angular parameters (ω, ϕ), the equivalence relations take the form:

$$(\omega, \beta) \sim \left(\omega - \frac{2\pi i}{n} + \frac{2\pi j}{m}, \beta - \frac{2\pi i}{n} \right); \quad i = 1, \ldots, n;\ j = 1, \ldots, m \tag{6}$$

Shown in Fig. 3 is the fundamental zone for complete boundary information for the $C_1 - C_2$ system. The torus is color coded to reflect the inherent symmetry and connectivity of the heterophase boundary space. In terms of topological properties, the heterophase boundary space can be embedded in $\mathbb{R}^3$ and has the non-trivial fundamental group $\mathbf{Z} \times \mathbf{Z}$ of the torus (Munkres 2000, 372).

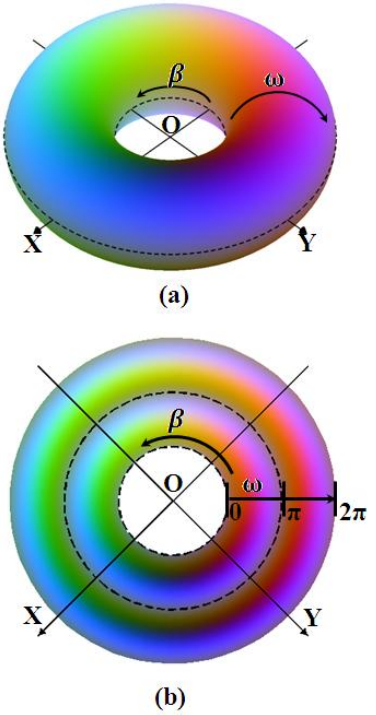

Figure 3: The heterophase boundary space of $\mathbf{C}_1 - \mathbf{C}_2$ system. The torus is colored such that the symmetry of the system $(\omega, \beta) \sim (\omega + \pi, \beta)$ is reflected. The symmetry is better captured when the system is projected onto a plane as shown in (b). The domain between the dotted lines, $\omega \in [0, \pi)$ and $\beta \in [0, 2\pi)$, represents the fundamental zone for this system.

4.3 Homophase Boundaries

The homophase boundary space is the quotient space of a torus with the following equivalence relations:

$$\begin{aligned}
&(\mathbf{i})\,(I, \mathbf{n}_1) \sim (I, \mathbf{n}_2) \\
&(\mathbf{ii})\,(\mathbf{M}, \mathbf{n}) \sim \left(\mathbf{M}^{-1}, \mathbf{M}^{-1}(-\mathbf{n})\right) \\
&(\mathbf{iii})\,(\mathbf{M}, \mathbf{n}) \sim \left(S_i^{-1}\mathbf{M}S_j, S_i^{-1}\mathbf{n}\right); \quad i, j = 1, \ldots, n
\end{aligned} \tag{7}$$

Here I refers to the zero misorientation. The equivalence relation 7(i) is referred to as the 'no-boundary' equivalence, the relation 7(ii) is the 'grain exchange symmetry' equivalence and the relations in 7(iii) arise due to the point symmetries of the

crystals. These equivalence relations expressed in terms of (ω,ω) take the form:

$$\begin{aligned}
&(i)\,(0,\beta_1)\sim(0,\beta_2)\\
&(ii)\,(\omega,\beta)\sim(2\pi-\omega,\pi-\omega+\beta)\\
&(iii)\,(\omega,\beta)\sim\left(\omega-\frac{2\pi i}{n}+\frac{2\pi j}{m},\beta-\frac{2\pi i}{n}\right);\ i,j=1,\ldots,n.
\end{aligned}\tag{8}$$

The no-boundary equivalence requires the collapse of the $\{\omega=0\}\times S^1$ region in the torus to a single point, which can be achieved by shrinking the inner radius of the torus to zero; see the difference between Fig. 4(a) and (b). This so-called 'horned torus' is equivalent to a 2-sphere with two antipodal points (the north and south poles) identified. The horned torus is mapped to a 2-sphere by expressing the polar coordinates in terms of the boundary parameters as $(\theta,\phi)=(\omega/2,\beta)$, which applies for the homophase boundaries of crystals with C_1 point symmetry. In the case of boundaries of crystals with C_n symmetry, the polar coordinates are related to the boundary parameters by the relation:

$$(\theta,\phi)=\left(\frac{n\beta}{2},n\omega\right)\tag{9}$$

where ω and β are restricted to $[0,2\pi/n]$. This ensures that θ is confined to $[0,\pi]$ and ϕ is confined to $[0,2\pi]$. In the domain $\omega,\omega\in[0,2\pi/n]$, the equivalence relations due to crystal symmetries need not be considered, which simplifies the subsequent analysis.

In polar coordinates the no-boundary equivalence relation takes the form $(0,\phi)\sim(\pi,\phi)$. This equivalence implies that the two poles, $(0,0,1)$ and $(0,0,-1)$ are identified. Even though the measure and metrics on a 2-sphere are familiar, the identification of the two poles makes the topology more complicated, and hence there is no immediately obvious method to define metrics. This singularity is a result of the 'no-boundary' condition at zero misorientation. We find, however, that this singularity can be removed by invoking grain exchange symmetry. Applying the equivalence relation from Equation 8(ii) to the polar coordinates of the 2-sphere results in the following equivalence relation:

$$\begin{aligned}
&\left(\frac{2\theta}{n},\frac{\phi}{n}\right)\sim\left(\frac{2\pi}{n}-\frac{2\theta}{n},\pi-\frac{2\theta}{n}+\frac{\phi}{n}\right)\\
&\Rightarrow\left(\theta,\frac{\phi}{n}\right)\sim\left(\pi-\theta,\frac{(\pi-2\theta)}{n}+\frac{\phi}{n}+\frac{(n-1)\,\pi}{n}\right)\\
&\Rightarrow(\theta,\phi)\sim(\pi-\theta,(\pi-2\theta)+\phi+(n-1)\,\pi)
\end{aligned}\tag{10}$$

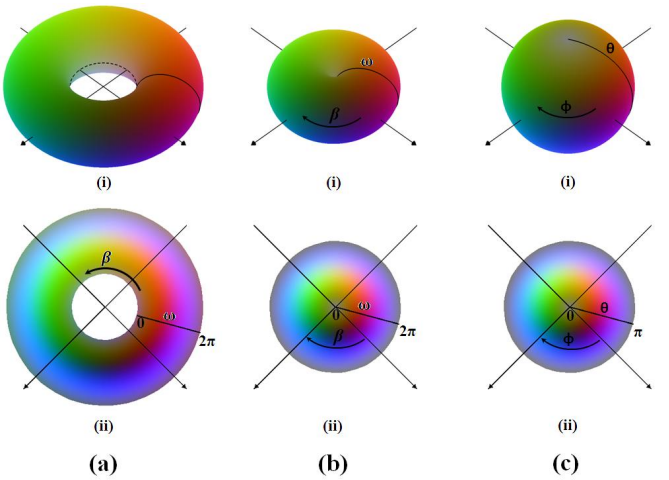

Figure 4: Colors are used to represents the connectivity of these spaces. (a) (i) $\mathbf{S}^1 \times \mathbf{S}^1$ torus and its (ii) projection onto a plane. (b) (i) The horned-tours (inner radius = 0) and its (ii) projection. As represented by the coloring scheme, the points $(\omega = 0, \beta)$ and $(\omega = 2\pi, \beta)$ are equivalent. (c) The horned-tours is mapped into a 2-sphere using the relation $(\theta, \phi) = (\mathbf{n}\omega/2, \mathbf{n}\beta)$.

This is a slightly complicated relation since the equivalence in the ϕ coordinate is dependent on θ. This complication can be removed by using modified parameters

$$(\theta', \phi') = \left(\theta, \phi - \frac{(\pi - 2\theta)}{2}\right) \tag{11}$$

which yields the following equivalence relation:

$$\begin{aligned} &\left(\theta', \phi' + \frac{(\pi - 2\theta)}{2}\right) \sim \left(\pi - \theta', \phi' + \frac{(\pi - 2\theta)}{2} + (n-1)\,\pi\right) \\ &\Rightarrow \left(\theta', \phi'\right) \sim \left(\pi - \theta', \phi' + (n-1)\,\pi\right) \end{aligned} \tag{12}$$

Two situations arise when the boundary parameters are expressed in terms of (θ', ϕ'). First, if n is odd, then the equivalence relation shown in Equation (12) is equivalent to $(\theta', \phi') \sim (\pi - \theta', \phi')$ (since $n-1$ is even and a multiple of 2π). Second, if n is even, then the equivalence relation is simplified to $(\theta', \phi') \sim (\pi - \theta', \phi' + \pi)$ (since $n-1$ is an odd number). The advantage of using the modified parameters in representing the boundary information is illustrated in Fig. 5 and Fig. 6 for odd- and even-fold rotational symmetry systems respectively. Using the modified

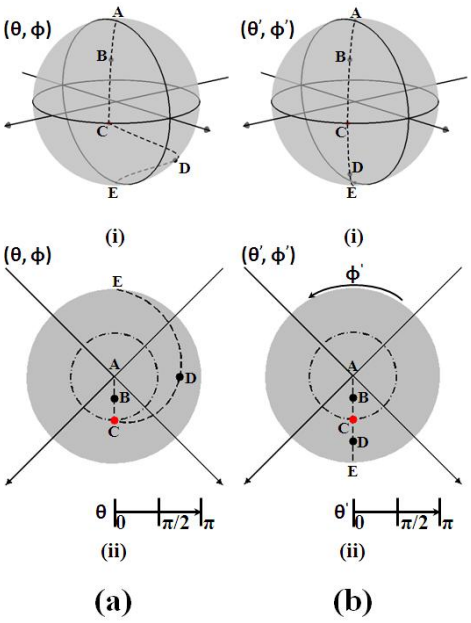

Figure 5: The equivalence relations corresponding to Equations (10) and (12) for odd-fold rotational symmetry systems (a) Homophase boundary information using (θ, ϕ) parameters. The path ABC in the upper hemisphere is equivalent to the path CDE in the lower hemisphere. This equivalence is better represented in its (ii) projection. (b) Boundary information using (θ', ϕ') parameters. In this parameterization the paths ABC and CDE are related through mirror symmetry.

parameters results in simple equivalence relations corresponding to either a mirror symmetry or an inversion symmetry on the 2-sphere.

To summarize, modified parameters (θ', ϕ') are used to represent the homophase boundary. They are related to boundary parameters by the following equation:

$$(\theta', \phi') = \left(\frac{n\omega}{2}, n\beta - \frac{(\pi - n\omega)}{2} \right) \tag{13}$$

where ω is restricted to $[0, 2\pi/n]$ and β is restricted to $[0, 2\pi/n\,]$. Any boundary with parameters $\omega > 2\pi/n$ or $\beta > 2\pi/n$ has a symmetrically equivalent description in the restricted domain, which is obtained by applying appropriate crystal symmetries. Examining the above results, we observe that the homophase boundary spaces of the C_1 and C_3 systems are topologically equivalent to that of a disc in the two-dimensional Euclidean plane. This is a result of the equivalence relation

$(\theta', \phi') \sim (\pi - \theta', \phi')$. This relation expressed in terms of Cartesian coordinates is of the form $(x, y, z) \sim (x, y, -z)$. Hence the topology of the homophase boundary space for these systems is the quotient space of the 2-sphere with the equivalence relation $(x, y, z) \sim (x, y, -z)$. This quotient space is equivalent to a disc $\left(D^2\right)$ in two-dimensional Euclidean plane. The space is *simply connected* (admits a trivial fundamental group) and can be embedded in $\mathbb{R}^2$.

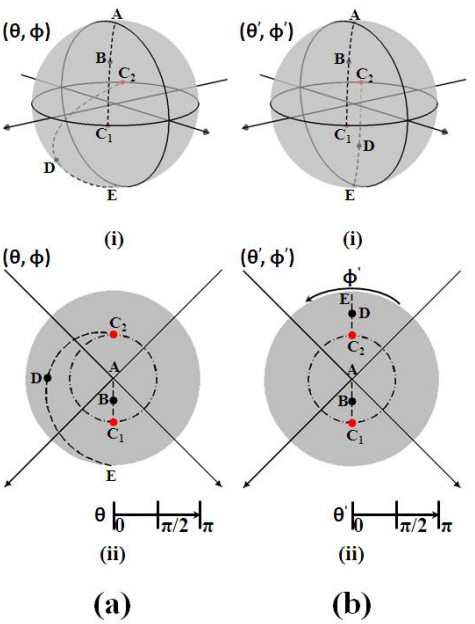

Figure 6: The equivalence relations corresponding to Equations (10) and (12) for even-fold rotational symmetry systems (a) Homophase boundary information using (θ, ϕ) parameters. The path ABC_1 in the upper hemisphere is equivalent to the path C_2DE in the lower hemisphere. This equivalence is better represented in its (ii) projection. (b) Boundary information using (θ', ϕ') parameters. In this parameterization the paths ABC_1 and C_2DE and are related by an inversion about the origin. The space is defined as the real projective plane $\left(\mathbb{R}\mathbf{P}^1\right)$.

In the case of the C_2, C_4 and C_6 systems (see Fig. 6) the boundary space is equivalent to the real projective plane $\left(\mathbb{R}P^2\right)$. The equivalence relation $(\theta', \phi') \sim (\pi - \theta', \phi' + \pi)$ expressed in terms of Cartesian coordinates is of the form $(x, y, z) \sim (-x, -y, -z)$, i.e. a 2-sphere with all antipodal points identified, or the real projective plane. The topological properties of $\mathbb{R}P^2$ are well documented. The minimum number of Euclidean dimensions in which it can be embedded is *four* (Kirby 2007).

It has a non-trivial fundamental group $\mathbf{Z}_2$ (Munkres 2000, 372)**.**

The parameterization in Equation (13) has several immediate practical consequences. For example, the metrics on a 2-sphere can be used to express the "distance" between homophase boundaries. This helps achieve meaningful answers to the question of how similar two boundaries are if they have different misorientations and boundary planes. The distance between two points denoted by (θ_1', ϕ_1') and (θ_2', ϕ_2') on a sphere is given by:

$$s = \arccos\left(\cos\theta_1' \cos\theta_2' + \sin\theta_1' \sin\theta_2' \cos\left(\phi_1' - \phi_2'\right)\right) \tag{14}$$

where $s \in [0, \pi]$.

The distance between two boundaries (ω_1, β_1) and (ω_2, β_2) is obtained in three steps:

(i) The evaluation of symmetrically equivalent descriptions of (ω_1, β_1) and (ω_2, β_2) that lie in the domain $[0, 2\pi/n]$.

(ii) Evaluation of symmetrically equivalent descriptions (mirror images for odd-fold rotation symmetry systems and antipodal points for even-fold rotation symmetry systems) of boundary parameters in the (θ', ϕ') parameterization using Equation 12.

(iii) The distance between the two boundaries is finally obtained by taking the minimum of the distances between the equivalent representations calculated using Equation 14.

Since the modified homophase grain boundary parameters (θ', ϕ') reside on the surface of a unit-sphere, functions describing distributions of these parameters can be expanded as a linear combination of the Laplace spherical harmonics Y_l^m (Nikiforov, Uvarov, and Boas 1988, 76) which form a complete set of orthonormal functions. Any square-integrable function can be expressed as a linear combination of the spherical harmonics as:

$$f\left(\theta', \phi'\right) = \sum_{l=0}^{\infty} \sum_{m=-l}^{l} C_l^m Y_l^m\left(\theta', \phi'\right) \tag{15}$$

It is necessary that the function f inherit the symmetries of the boundary space. This is achieved by using symmetrized spherical harmonics which are commonly used in pole distributions in representing texture (Popa 1992). Symmetrized spherical harmonics must reflect the mirror symmetry in the case of C_1 and C_3 boundary systems and the inversion symmetry in the case of C_2, C_4 and C_6 boundary systems.

5 Conclusions

The grain exchange symmetry $(\mathbf{M},\mathbf{n}) \sim \left(\mathbf{M}^{-1},\mathbf{M}^{-1}(-\mathbf{n})\right)$ has profound implications for the topology of homophase misorientations and the complete homophase grain boundary space. Here we have shown that for 2-D systems, this symmetry simplifies the apparently complex topology of both of these spaces.

In the case of homophase misorientation spaces, the equivalence relation due to grain exchange symmetry reduces the embedding dimensions of the misorientation space; here we show a reduction from two for rotations, to one for misorientations. When the grain exchange symmetry is applied to the complete homophase boundary space in two-dimensional systems, the complication due to the 'no-boundary' singularity is removed. Parameters (θ',ϕ') are used to represent the homophase boundary parameters and the topology of the boundary space expressed using this parameterization is the quotient space of a 2-sphere $\left(S^2\right)$. As a result of this finding, the round metric on the sphere may be used to define distances between homophase boundaries, and symmetrized hyperspherical harmonics can be used to express homophase boundary distributions.

Our analysis of two-dimensional systems reveals a critical and previously unappreciated role of grain exchange symmetry in understanding the topology of the complete boundary space, and provides a basis for investigating the topology of homophase boundaries for three-dimensional crystals.

Acknowledgement: This work was supported by the US National Science Foundation, under contract DMR-0855402.

References

Argon, A. S., Qiao, Y. (2002): Cleavage cracking resistance of large-angle grain boundaries in Fe-3 wt% Si alloy. *Philosophical Magazine A* 82, no. 17: 3333–3347.

Aust, K. T., Erb, U., Palumbo, G. (1994): Interface control for resistance to intergranular cracking. *Materials Science and Engineering*: A 176, no. 1-2: 329–334.

Basener, W. F. (2006): *Topology and its applications*. Wiley-Interscience.

Cahn, J. W., Taylor, J. E. (2006): Metrics, measures, and parametrizations for grain boundaries: a dialog. *Journal of Materials Science* 41, no. 23: 7669–7674.

Groeber, M. A., Haley, B. K., Uchic, M. D., Dimiduk, D. M., Ghosh, S. (2006): 3D reconstruction and characterization of polycrystalline microstructures using a FIB-SEM system. *Materials Characterization* 57, no. 4-5: 259–273.

Heinz, A., Neumann, P. (1991): Representation of orientation and disorientation

data for cubic, hexagonal, tetragonal and orthorhombic crystals. *Acta Crystallographica Section A: Foundations of Crystallography* 47, no. 6: 780–789.

Ju, S., Sun, H., Li, Z. Y. (2002): Study of magnetotransport in polycrystalline perovskite manganites. *Journal of Physics: Condensed Matter* 14, no. 38: L631–L639.

Kim, C. S., Rollett, A. D., Rohrer, G. S. (2006): Grain boundary planes: New dimensions in the grain boundary character distribution. *Scripta materialia* 54, no. 6: 1005–1009.

Kirby, R. (2007): Communications-WHAT IS... Boy's Surface? *Notices of the American Mathematical Society* 54, no. 10: 1306–1307.

Kokawa, H., Shimada, M., Michiuchi, M., Wang, Z. J., Sato, Y. S. (2007): Arrest of weld-decay in 304 austenitic stainless steel by twin-induced grain boundary engineering. *Acta Materialia* 55, no. 16: 5401–5407.

Kraft, R. H., Molinari, J. F. (2008): A statistical investigation of the effects of grain boundary properties on transgranular fracture. *Acta Materialia* 56, no. 17: 4739–4749.

Lim, L. C., Watanabe, T. (1990): Fracture toughness and brittle-ductile transition controlled by grain boundary character distribution (GBCD) in polycrystals. *Acta Metallurgica et Materialia* 38, no. 12: 2507–2516.

Morawiec, A. (2004): *Orientations and rotations: computations in crystallographic textures*. Springer Verlag.

Morawiec, A. (2009): Models of uniformity for grain boundary distributions. *Journal of Applied Crystallography* 42, no. 5.

Munkres, J. R. (2000): *Topology*. Prentice Hall.

Nikiforov, A. F., Uvarov, V. B., Boas, R. P. (1988): *Special functions of mathematical physics*. Birkhäuser Basel.

Olmsted, D. L. (2009): A new class of metrics for the macroscopic crystallographic space of grain boundaries. *Acta Materialia* 57, no. 9: 2793–2799.

Olmsted, D. L., Foiles, S. M., Holm, E. A. (2009): Survey of computed grain boundary properties in face-centered cubic metals: I. Grain boundary energy. *Acta Materialia* 57, no. 13: 3694–3703.

Olmsted, D. L., Holm, E. A., Foiles, S. M. (2009): Survey of computed grain boundary properties in face-centered cubic metals—II: Grain boundary mobility. *Acta Materialia* 57, no. 13 (8): 3704-3713. doi:10.1016/j.actamat.2009.04.015.

Popa, N. C. (1992): Texture in Rietveld refinement. *Journal of Applied Crystal-*

lography 25, no. 5 (10): 611-616. doi:10.1107/S0021889892004795.

Rohrer, G. S., Saylor, D. M., Dasher, B. El., Adams, B. L., Rollett, A. D., Wynblatt, P. (2004): The distribution of internal interfaces in polycrystals. *Zeitschrift fur Metallkunde* 95, no. 4: 197–214.

Rowenhorst, D. J., Gupta, A., Feng, C. R., Spanos, G. (2006): 3D crystallographic and morphological analysis of coarse martensite: combining EBSD and serial sectioning. *Scripta materialia* 55, no. 1: 11–16.

Spowart, J. E. (2006): Automated serial sectioning for 3-D analysis of microstructures. *Scripta materialia* 55, no. 1: 5–10.

Uchic, M. D., Groeber, M. A., Dimiduk, D. M., Simmons, J. P. (2006): 3D microstructural characterization of nickel superalloys via serial-sectioning using a dual beam FIB-SEM. *Scripta materialia* 55, no. 1: 23–28.

Watanabe, T. (1994): The impact of grain boundary character distribution on fracture in polycrystals. *Materials Science and Engineering*: A 176, no. 1-2: 39–49.